J Solid State Electrochem (2012) 16:2143–2149
DOI 10.1007/s10008-011-1634-y

ORIGINAL PAPER

Electrochemical monitoring of photoelectrocatalytic degradation of rhodamine B using TiO_2 thin film modified graphite electrode

Reza Ojani · Jahan-Bakhsh Raoof · Ebrahim Zarei

Received: 8 August 2011 / Revised: 21 December 2011 / Accepted: 25 December 2011 / Published online: 11 January 2012

Abstract A commercially available TiO_2 powder (Degussa P25) has been used to prepare thin films on graphite plates. The photoelectrochemical degradation of rhodamine B was investigated using this photoelectrode. The effects of applied potential, pH, and initial rhodamine B concentration on the photoelectrocatalytic (PEC) degradation of rhodamine B using ultraviolet illuminated TiO_2/graphite (TiO_2/C) thin film electrode were examined and discussed. Also, direct photolysis, electrochemical oxidation, photocatalytic, and PEC degradation of rhodamine B were compared. Results show that the best responses for PEC are obtained at applied potential of 1.2 V vs. reference electrode, pH 4.0, and initial rhodamine B concentration of 4.2 mg L^{-1}.

Keywords Photoelectrocatalysis · Titanium dioxide · Graphite plates · Rhodamine B

Introduction

Since the first photocatalytic oxidation study for treating organic contaminants in wastewater was carried out by Carey in 1976 [1, 2], many research reports have shown that the semiconductor TiO_2 is an excellent photocatalyzer which can break down many kinds of refractory organic pollutants, such as detergents, dyes, pesticides, and herbicides, etc., under UV light irradiation [3–11]. However, there are two inherent problems in using TiO_2 particle suspensions for toxic water remediation such as the difficulty of separating and recovering the photocatalyst particles from the aqueous phase and the very low quantum yield [12] due to high degree of recombination between photogenerated charge carriers (electron and holes), in which TiO_2 particles behave as short-circuited microelectrodes under band gap excitation [13]. To solve the problems of TiO_2 particle separation from wastewater, many efforts and attempts were done by researchers in trying to immobilize TiO_2 film on a solid carrier such as sand, glass media, or resins by coating, soaking, precipitating, or spinning methods. However, while these immobilized TiO_2 photooxidation processes made the TiO_2 separation from water phase much easier, they did not achieve any improvement in quantum efficiency. Then on the basis of immobilized TiO_2 photocatalytic (PC) oxidation, researchers carried out photoelectrocatalytic (PEC) oxidation by applying a positive potential bias to TiO_2 film [14–21]. The externally applied anodic bias can withdraw the excited electrons to a counter electrode and results in a decrease in the recombination rate of photogenerated electrons and holes. On the other hand, rhodamine B is one of the most common xanthene dyes for textile industry. It is famous for its good stability as dye laser materials, and it is also used as a biological stain. Rhodamine B is highly soluble in water and organic solvent, and its color is fluorescent bluish-red. In addition, rhodamine B is used in many industrial processes, such as paper dyeing and dye laser production [22]. This compound is now banned from use in foods and cosmetics because it has been found to be potentially toxic and carcinogenic, therefore degradation of rhodamine B is a matter of great interest [23, 24].

In this study, a TiO_2/graphite (TiO_2/C) thin film electrode was produced by suspending a known amount of the Degussa P25 suspensions to a surface of graphite plates. This electrode was employed for PEC oxidation of

R. Ojani (✉) · J.-B. Raoof · E. Zarei
Electroanalytical Chemistry Research Laboratory,
Faculty of Chemistry, University of Mazandaran,
Babolsar, Iran
e-mail: fer-o@umz.ac.ir

rhodamine B under UV irradiation. In this work, the influence of various parameters (such as pH value of solution, initial rhodamine B concentration, and electrical bias value applied) was investigated on PEC degradation of rhodamine B.

Experimental

Materials

The solvent used for the electrochemical studies was doubly distilled water. The rhodamine B from Merck was used as received. High viscosity paraffin (density, 0.88 $g cm^{-3}$) from Fluka and graphite powder (particle diameter, 0.10 mm) from Merck were used for the preparation of working electrode. Graphite electrodes were cut from a graphite plate. TiO_2 powder (product name P25, particle size 30 nm, surface area 50 m^2/g) was purchased from Degussa Corp. The major fraction of this sample consists of Anatase form of TiO_2. Buffer solutions were prepared from NaOH, H_3PO_4, and phosphate salts for the pH range of 3.0–11.0.

Preparation of working electrode

TiO_2 films were coated from a TiO_2 suspension using dip-coating technique. This suspension was prepared by suspending a known amount of the Degussa P25 powder in water (250 g/L) and sonicating it for 30 min. For the preparation of TiO_2 film, a graphite plate (3.0×3.0 cm^2) was dipped into the TiO_2 suspension for 15 s and then lifted up and preheated at 90 °C. The method from dipping to preheating was repeated for six cycles. Then, the electrode was sintered at 400 °C for 1 h. The semiconductor thin film sintered at 400 °C adhered strongly to the graphite surface and was stable in the pH range of 1–13.

Instrumentation

PEC degradation experiments were carried out in a single photoreactor consists of a quartz cylindrical cell (3.0-cm diameter × 8.0-cm height, 1.8-mm thick) as shown in Fig. 1. The reactor and the UV lamp were placed in a black box in order to avoid extraneous illumination. A platinum rod as a counter electrode and an Ag|AgCl|KCl (3 M) as a reference electrode were used. TiO_2/C was applied as a working electrode for performing the processes of PEC and electrochemical oxidation (EC) degradation and as a surface photocatalyst for performing the process of PC degradation of rhodamine B. Photoelectrochemical and electrochemical experiments were carried out using a potentiostat/galvanostat (μ-Autolab Type III). A carbon paste electrode was used as a working electrode for the

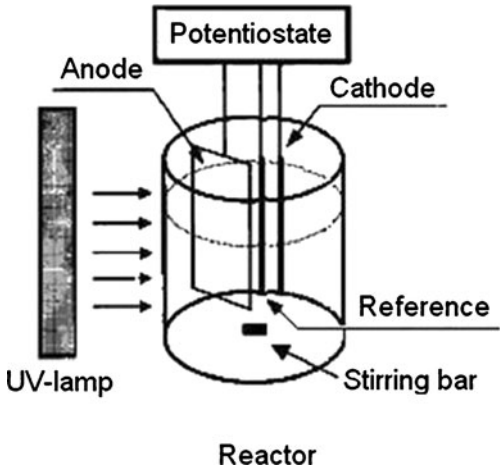

Fig. 1 Schematic diagram of the reactor system

electrochemical monitoring of rhodamine B concentration variations in the different experiments such as PEC degradation. The said monitoring was carried out over different times by measuring the peak current (I_p) decay at the peak potential (E_p) oxidation of rhodamine B using differential pulse voltammetry method as an electrochemical monitoring method. A collimated light beam from a 4-W medium pressure mercury lamp with a maximum UV irradiation peak was used for the excitation of photoelectrode.

Results and discussions

Scanning electron microscopy of the TiO_2/C electrode

Figure 2 shows a typical SEM image of the TiO_2-modified graphite electrode. It can be seen from the micrograph that spherical TiO_2 particles were distributed uniformly on the surface of graphite and that the average size is almost the same as that of the original Degussa P25 TiO_2.

Photoelectrochemical properties of the TiO_2/C electrode

In photocatalysis process, when the TiO_2 nanoparticles in colloidal suspensions or deposited as a thin film on a solid carrier were illuminated with UV light, a great number of electrons would be excited from the valence band (VB) to the conduction band (CB) by absorbing UV light quanta, leaving highly oxidative holes in VB (h_{VB}^+) and forming negative sites in CB (e_{CB}^-), as shown in Fig. 3a(1) and reaction (1) [25]:

$$TiO_2 + hv \rightarrow e_{CB}^- + h_{VB}^+ \quad (1)$$

Organics can then be directly oxidized by the hole or by the heterogeneous hydroxyl radical formed from the

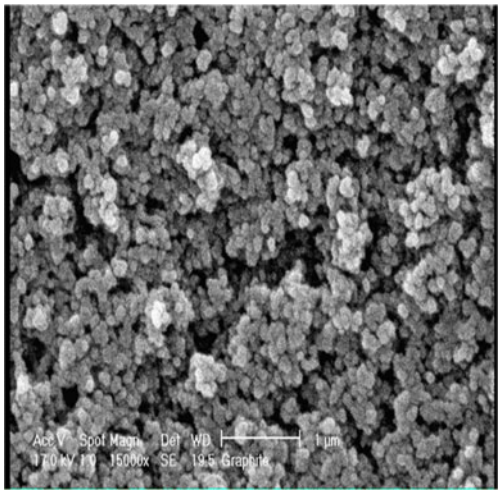

Fig. 2 SEM micrograph of TiO_2/C electrode

following reaction between the photogenerated vacancy and adsorbed water:

$$h_{VB}^{+} + H_2O \rightarrow {}^{\bullet}OH + H^{+} \quad (2)$$

In addition, other weaker oxidizers (superoxide radical ion $O_2^{\bullet-}$, $HO_2^{\bullet}$, and H_2O_2) and more $^{\bullet}OH$ can be produced from the photoinjected electron by the following reactions [25]:

$$e_{CB}^{-} + O_2 \rightarrow O_2^{\bullet-} \quad (3)$$

$$O_2^{\bullet-} + H^{+} \rightarrow HO_2^{\bullet} \quad (4)$$

$$2HO_2^{\bullet} \rightarrow H_2O_2 + O_2 \quad (5)$$

$$H_2O_2 + O_2^{\bullet-} \rightarrow {}^{\bullet}OH + OH^{-} + O_2 \quad (6)$$

The major loss in efficiency of photocatalysis is due to the recombination of electrons promoted to the valence band either with unreacted holes or with adsorbed hydroxyl radicals as observed in Fig. 3a(2) and in the following reactions [26]:

$$e_{CB}^{-} + h_{VB}^{+} \rightarrow TiO_2 + heat \quad (7)$$

$$e_{CB}^{-} + {}^{\bullet}OH \rightarrow OH^{-} \quad (8)$$

The electrochemical technology can provide much higher efficiency for organic material oxidation by means of photoelectrocatalysis. The efficiency of this process was improved by applying a suitable anodic potential to the circuit owing to the conducting graphite substrate. The application of an anodic bias to a TiO_2/C electrode further provides a potential gradient within the film to drive away the photogenerated holes and electrons in different directions efficiently. The photogenerated holes could oxidize the organic compounds at the anode surface (Fig. 3a(3)), while the photogenerated electrons were transferred to the acceptor at the metallic cathode through the external electrical circuit (Fig. 3a(4)). As indicated in Fig. 3b, thin semiconductor particulate films prepared from particulate suspensions are consist of small particles which are in close contact with each other and are capable of exhibiting photoelectrochemical properties similar to polycrystalline semiconductor films. The whole reaction process viewed on both macroscopic and microscopic scales was shown in Fig. 3.

To study the photoelectrochemical response of TiO_2/C electrode, hydrodynamic amperometry was used in buffer solution in the presence and absence of methanol under UV irradiation. The results are shown in Fig. 4. It can be seen that the rise and fall of the photocurrent corresponded well to the illumination being switched on and off. The

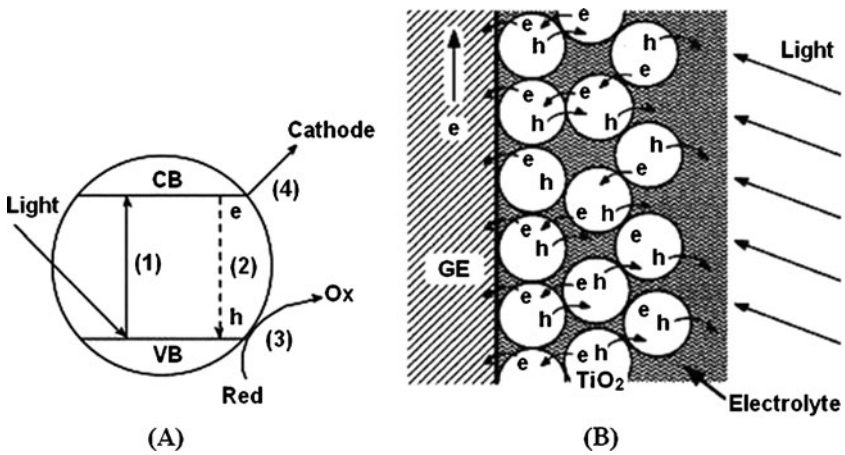

Fig. 3 Schematic representation of photocurrent generation from the microscopic (**a**) and macroscopic (**b**) views

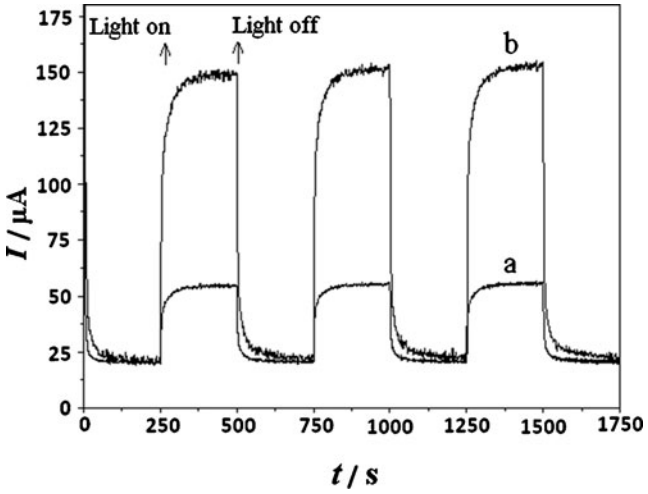

Fig. 4 Hydrodynamic amperograms of TiO_2/C electrode in phosphate buffer solution (pH 7.0) in the absence (**a**) and presence (**b**) of 3.0 mg L^{-1} methanol together with several on–off cycles irradiation. External bias 0.5 V

generation of photocurrent consisted of two steps. The first step of the photocurrent appears promptly after the illumination, and the second step of the photocurrent reaches a steady state. This pattern of photocurrent is highly reproducible for several on–off cycles of illumination. The current response on the TiO_2/C electrode is insignificant which means that no electrochemical oxidation occurred. Under illumination, a significant increase in the photocurrent is observed. This indicates that photogenerated electrons on TiO_2/C electrode could be effectively driven to the counter electrode by applied positive potential, which would be beneficial to charge separation. In buffer solution, the photogenerated holes in TiO_2/C electrode oxidize either adsorbed water molecules or hydroxyl groups, while the presence of methanol provides a much more facile pathway for the transfer of holes across the film/electrolyte interface, which results in the higher photocurrent.

Comparison of different degradation processes of rhodamine B

The remarkable synergistic effect of a biased photoanode on the photocatalytic process during the discoloration of a 4.2 mg L^{-1} rhodamine B dye solution in phosphate buffer solution (pH 7.0) was observed in Fig 5a. The relative concentration of rhodamine B, C/C_o, is considered in this figure and in other figures as a fractional conversion of rhodamine B and is plotted in a time-dependent scale. The fractional conversion was obtained by evaluating the ratio of rhodamine B concentration C at time t and the initial rhodamine B concentration C_o in the solution at t=0. Four distinct conditions were investigated: (a) the photoelectrocatalytic process using both UV light and E=0.65 V, (b) the photocatalytic process using UV light without a bias potential, (c) the direct photolysis (DC) process using UV light without a bias potential, and (d) the electrochemical oxidation process applying E=0.65 V in dark conditions. In all cases, TiO_2/C electrode was applied except in the direct photolysis process. The experimental results shown in Fig. 5a demonstrated that the removal rate of rhodamine B in the PEC oxidation was more than that in the PC, DP, and EC oxidation. Also, the results illustrate that dye degradation by photoelectrocatalytic procedures is more effective than the expected summation of electrochemical degradation and photocatalytic effects. Instead, a synergistic effect seems to play a major role in the final treatment. Applying a bias potential significantly increases the efficiency of the photocatalytic activity of the TiO_2/C electrode and thereby increases the reaction rate of dye oxidation.

Figure 5b shows the differential pulse voltammograms of rhodamine B at various times at the surface of carbon paste

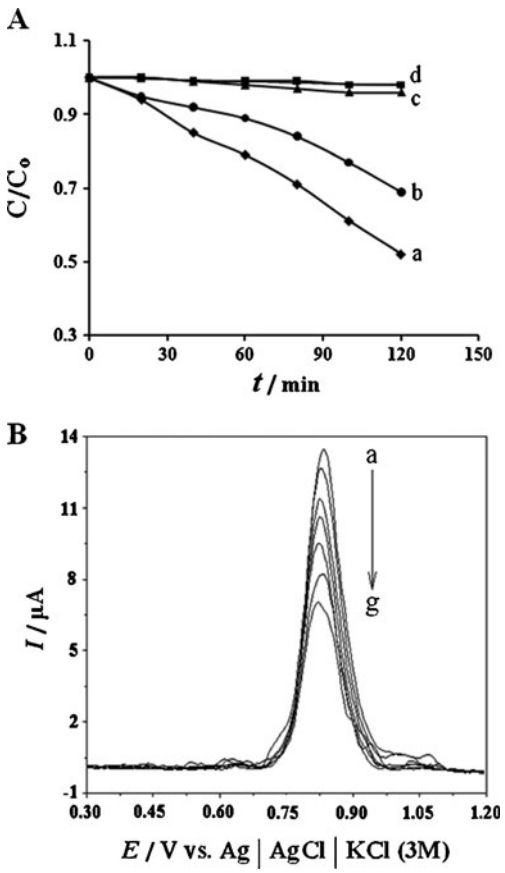

Fig. 5 **a** Comparison of (*a*) PEC, (*b*) PC, (*c*) DC, and (*d*) EC degradation of rhodamine B. Phosphate buffer solution (pH 7.0), initial rhodamine B concentration 4.2 mg L^{-1}, and external bias 0.65 V. **b** Differential pulse voltammograms of rhodamine B in PEC degradation process at the surface of the carbon paste electrode in PEC degradation process at various times: (*a*) 0, (*b*) 20, (*c*) 40, (*d*) 60, (*e*) 80, (*f*) 100, and (*g*) 120 min. Scan rate 10 mV s^{-1}

electrode for PEC process as an example. Rhodamine B concentration variations were determined by monitoring the I_p value at the E_p oxidation of rhodamine B over different times. From Fig. 5b, it can be clearly seen that the peak current decreases as a function of time during photoelectrocatalysis. This means that rhodamine B disappeared quickly with the increase of reaction time in PEC degradation process. The Langmuir–Hinshelwood kinetic model formula has usually been applied to describe the photocatalytic and photoelectrocatalytic reactions. In this study, the experimental results can well fit the first-ordered reaction model equation, $\ln(C_o/C)=f(t)=kt$ (k is a rate constant). The corresponding reaction rate constant k can be obtained from the degradation efficiency of rhodamine B. These rate constants were listed in Table 1. The experimental results demonstrated that the reaction rate of rhodamine B degradation in the PEC process was faster than that in the PC, DP, and EC processes.

Effect of initial pH value

In water or wastewater treatment, pH is a common factor that influences the removal of pollutants in many processes of charged organic pollutants because the pH value of the solution will change the existed configuration of degraded species and surface charges of catalysts. The relationship between pH value and removal efficiency of the PEC degradation of rhodamine B was studied (Fig. 6). These results were obtained with initial rhodamine B concentration of 4.2 mg L^{-1} over 1-h illumination at bias potential of 0.65 V vs. reference electrode. As shown in this figure, rhodamine B degradation kinetics are optimal at pH 4.0 compared with other pHs. Also, we can easily see that the amount of rhodamine B degraded decreases sharply to pH 4, but after a decrease to pH 5, it is almost constant to pH 8 and then decreases sharply after that to pH 9.

Since the isoelectrical point of TiO_2 is at pH 4–6, hence, the catalyst surface is positively charged at more acidic pH, while it is negatively charged at pH value almost above 6 [27]. Also, the value of pH could influence the charge carried by the molecule of rhodamine B (pK_a=3.7) as shown in Fig. 7. When the pH value was less than 4, the molecule of rhodamine B was in the cationic form, and its adsorption on the catalyst surface became difficult because of an electrostatic repulsive force. When the pH value was greater than 4, the carboxyl group of rhodamine B molecule loosed its proton, and therefore, this molecule was in the zwitterionic form. Subsequently, a certain part of the molecule was attracted by the catalyst surface due to the electrostatic attraction [28]. The rhodamine B degradation showed its maximum at pH 4, and it was almost constant from pH 5 to pH 8. This reason may be attributed to the greater attraction of rhodamine B at the surface of TiO_2/C electrode because PEC degradation of rhodamine B occurred at the interface of the electrode and solution. This means that at pH 4, the amount of rhodamine B attracted at the surface of TiO_2/C electrode was maximum, and this amount at pH 5–8 was almost constant and smaller than that of pH 4. Of course, the pH value influences the PEC process in many other ways, such as the easy adsorption of the active species like elemental oxygen at the isoelectric point because of the neutral surface charges [3] and reduction potential of TiO_2 valence band variation [29]. However, when pH is over 9, an increase of removal rate was observed in our experiment. The reason may be that under the strong alkaline condition, rhodamine B would lose protons and would then be easily oxidized. Meanwhile, in alkaline medium, there are large quantities of hydroxyl radicals with strong oxidizing ability [30].

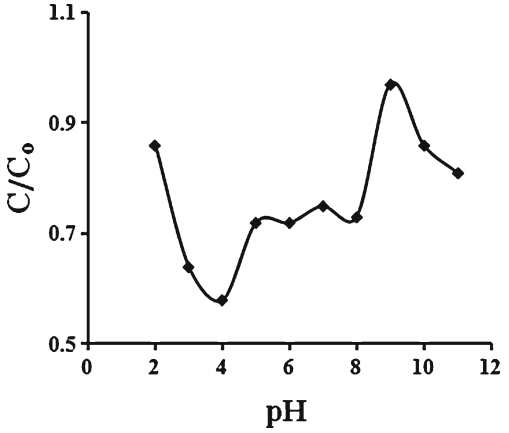

Fig. 6 Effect of pH value of solution on PEC degradation of rhodamine B. Initial rhodamine B concentration 4.2 mg L^{-1}, external bias 0.65 V, and time experiment 60 min

Table 1 Comparison of rate constants k (calculated based on the data in Fig. 5a) degradation of rhodamine B with PEC, PC, DP, and EC degradation processes

Process	Rate constant, k (min^{-1})	Correlation coefficient, R
PEC	0.0053	0.9876
PC	0.0029	0.9720
DP	0.0004	0.9574
EC	0.0003	0.9701

Effect of initial rhodamine B concentration

Figure 8 shows the effects of initial rhodamine B concentration on degradation. The amount of the PEC degradation of rhodamine B increased, but the removal rate decreased

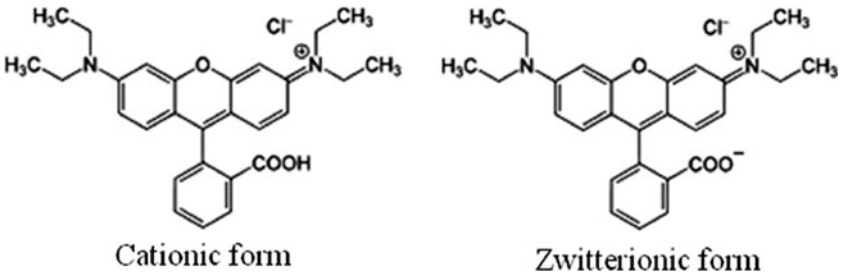

Fig. 7 Molecular structure of rhodamine B

with the increase of initial rhodamine B concentration. This phenomenon was related with the number of the catalysts surface adsorption positions. Since the PEC oxidation took place on the catalyst surface, not in the bulk of the solution [31], the accumulation of the adsorbate (rhodamine B or the intermediates) on the surface of the electrode may result in a decline of degradation rate.

Effect of applied potentials

The bias potential is an important factor in the process of PEC degradation of rhodamine B. Bias potential that ranged between 0.4 and 1.4 V were monitored over 90 min (Fig. 9). The results demonstrated that the amount of rhodamine B degraded was increased with the increase of potential. We believe this to be due to the decrease in the electron–hole recombination rate. The application of positive potential across the graphite plate-supported TiO_2 photoelectrode could produce a potential gradient inside the film that forced the photogenerated holes and electrons to move in opposite directions. Subsequently, the concentration of photogenerated holes (or hydroxyl radicals formed by subsequent oxidation of water) on the surface increased which, in turn, caused the amount of rhodamine B degraded to increase. Most of the photogenerated electrons were removed either by the electric field or by reaction with dissolved oxygen. Further increasing the applied potential beyond 1.2 V leads to a slight decrease in rhodamine B degradation. This can be explained by the fact that more water was oxidized by photogenerated holes [32]. Bias potential of 1.2 V was selected as optimal bias potential for PEC degradation of rhodamine B solution.

Conclusion

This study demonstrated that TiO_2 coatings on graphite plate provided suitable materials for constructing PEC reactors for rhodamine B degradation. The advantage of combining photocatalysis with electrochemistry, by applying positive potentials across the photoelectrode, has been confirmed. Also, it was found that the pH value of solution, initial rhodamine B concentration, and voltage of the electrical bias applied obviously have an influence on the degradation of rhodamine B. Such a beneficial aspect of electrochemically assisted photocatalysis can find its application in photocatalytic reactors with immobilized semiconductor particles.

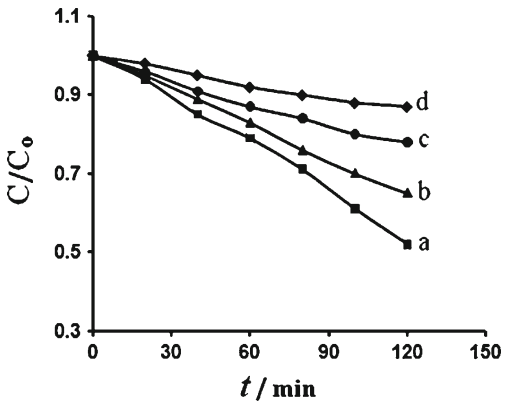

Fig. 8 Effect of different initial rhodamine B concentration on rhodamine B degradation: (*a*) 4.2, (*b*) 6.2, (*c*) 8.2, and (*d*) 10.2 mg L^{-1}. Phosphate buffer solution (pH 4.0) and external bias 0.65 V

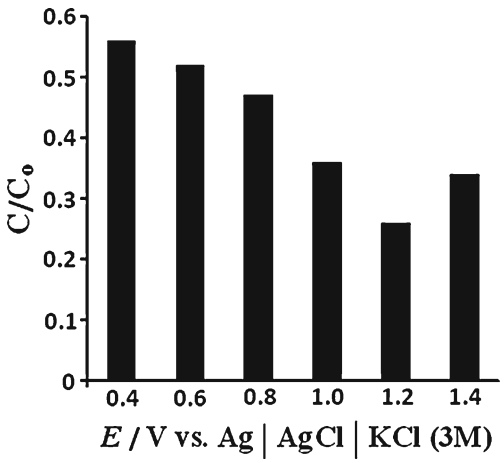

Fig. 9 Effect of different applied potentials on degradation of rhodamine B. Phosphate buffer solution (pH 4.0), initial rhodamine B concentration 4.2 mg L^{-1}, and time experiment 90 min

References

1. Carey JH (1976) Bull Environ Contam Toxicol 16:663–667
2. Aurian V (1988) Toxicol Environ Chem 16:89–109
3. Li XZ, Li FB (2001) Environ Sci Technol 35:2381–2387
4. Li FB, Li XZ, Hou MF (2004) Appl Catal B Environ 48:185–194
5. Armon R, Weltch-Cohen G, Bettane P (2004) Wat Sci Technol 4:7–14
6. Lee JP, Kim HK, Park CR, Park G, Kwak HT, Koo SM, Sung MM (2003) J Phys Chem B 107:8997–9002
7. Hachem C, Bocquillon F, Zahraa O, Bouchy M (2001) Dyes Pigments 49:117–125
8. Wang Y (2000) Water Res 34:990–994
9. Leng WH, Zhang Z, Zhang JQ (2003) J Mol Catal A Chem 206:239–252
10. Chen XB, Mao SS (2007) Chem Rev 107:2891–3041
11. Mandal SS, Bhattacharyya AJ (2010) Talanta 82:876–884
12. Choi W, Termin A, Haffmann MR (1994) J Phys Chem 98:13669–13679
13. Kormann C, Bahnmann DW, Haffmann MR (1991) Environ Sci Technol 25:494–500
14. Li MC, Shen JN (2006) J Solid State Electrochem 10:980–986
15. Qian X, Qin D, Bai Y, Li T, Tang X, Wang E, Dong S (2001) J Solid State Electrochem 5:562–567
16. Li XZ, Li FB, Fan CM, Sun YP (2002) Water Res 36:2215–2224
17. Jiang D, Zhao H, Zhang S, John R, Will GD (2003) J Photochem Photobiol A Chem 156:201–206
18. Zhang Z, Yuan Y, Shi G, Fang Y, Liang L, Ding H, Jin L (2007) Environ Sci Technol 41:6259–6263
19. Jorge SMA, Sene JJ, Florentino AO (2005) J Photochem Photobiol A Chem 174:71
20. Zhou M, Ma X (2009) Electrochem Commun 11:921–924
21. Diang D, Zhao H, Jia Z, Cao J, John R (2001) J Photochem Photobiol A Chem 144:197
22. Soares ET, Lansarin MA, Moro CC (2007) Braz J Chem Eng 24:29–36
23. Shang J, Zhang Y, Zhu T, Wang Q, Song H (2011) Appl Catal B Environ 102:464–469
24. Li J, Li L, Zheng L, Xian Y, Jin L (2006) Electrochim Acta 51:4942–4949
25. Xie YB, Li XZ (2006) Mater Chem Phys 95:39–50
26. Peralta-Hernandez JM, Meas-Vong Y, Rodriguez FJ, Chapman TW, Maldonado MI, Godinez LA (2006) Water Res 40:1754–1762
27. Kim DH, Anderson MA (1996) J Photochem Photobiol A Chem 94:221–229
28. Guo Y, Zhao J, Zhang H, Yang S, Qi J, Wang Z, Xu H (2005) Dyes Pigments 66:123–128
29. Lu MC, Roam GD, Chen JN, Huang CP (1996) Water Res 30:1670–1676
30. Leng WH, Liu H, Cheng SA, Zhang JQ, Cao CN (2000) J Photochem Photobiol A Chem 131:125–132
31. Kim DH, Anderson MA (1994) Environ Sci Technol 28:479–483
32. Hitchman ML, Tian F (2002) J Electroanal Chem 538–539:165–172